Far-field Drag Extraction from Hybrid Grid Computations

D.Destarac

ONERA

(in the framework of an Airbus-DLR-ONERA cooperation)

Acknowledgements

The new form of the theory of near-field / far-field drag balance used here is due to Jaap van der Vooren, retired, formerly NLR.

The presentation is taken charge of by Sébastien Esquieu, PhD Student, ONERA / Université de Bordeaux.

Drag extraction: near-field drag, far-field drag, near-field / far-field drag bala

near-field drag:

- *integration of the stresses at the surface of the aircraft*
- *provides the mechanical breakdown: pressure drag + friction drag*

far-field drag:

- *integrals derived from the momentum theorem, involving control volumes or surfaces within the flow field*
- *provides the physical breakdown: viscous drag + wave drag + induced drag*

near-field / far-field drag balance:

J. van der Vooren's far-field drag formulation ensures an exact near-field / far-field drag balance:

$$CDp + CDf = CDv + CDw + CDi$$

Van der Vooren's new formulation for the far-field drag components

Field quantities involved in the formulation:

$$\Delta\overline{u} = u_\infty\sqrt{1 + 2\frac{\Delta H}{{u_\infty}^2} - \frac{2}{(\gamma-1){M_\infty}^2}[(e^{\frac{\Delta s}{R}})^{\frac{\gamma-1}{\gamma}} - 1]} - u_\infty$$

$$\vec{f}_{vw} = -\rho\Delta\overline{u}\vec{q} \qquad \vec{f}_i = -\rho(u - u_\infty - \Delta\overline{u})\vec{q} - (p - p_\infty)\vec{i} + \vec{\tau}_x$$

Van der Vooren's new formulation for the far-field drag components

The theory is based on the assumption that production of viscous drag and wave drag is confined to finite non overlapping control volumes V_V (boundary layers and viscous shear layers) and V_W (shock layers), and that the flow can be considered as inviscid outside these volumes.

The far-field drag components can then be expressed as:

$$D_v = \int_{V_V} div\,\vec{f}_{vw} dV \qquad D_w = \int_{V_W} div\,\vec{f}_{vw} dV \qquad D_i = \int_{V_V+V_W} div\,\vec{f}_i dV - \int_{S_A} (\vec{f}_i.\vec{n}) dS$$

(S_A being the aircraft surface, $\vec{n}$ oriented from the flow-field toward the body.)

This formulation requires no small disturbance assumption and ensures an exact near-field / far-field drag balance:

$$D_p + D_f = D_v + D_w + D_i$$

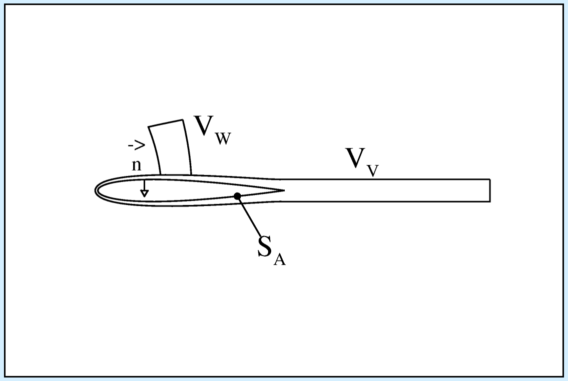

Accounting for spurious phenomena:

1) Spurious drag production

If spurious viscous or wave drag is generated in V_{SP} by the numerical technique used to solve the equations, outside the volumes V_V and V_W where viscous or wave drag production is physically justified, the near-field / far-field drag balance becomes

$$D_p + D_f = D_v + D_w + D_{sp} + D_i$$

with

$$D_v = \int_{V_V} div\,\vec{f}_{vw} dV \qquad D_w = \int_{V_W} div\,\vec{f}_{vw} dV \qquad D_{sp} = \int_{V_{SP}} div\,\vec{f}_{vw} dV$$

and

$$D_i = \int_{V_V+V_W+V_{SP}} div\,\vec{f}_i dV - \int_{S_A} (\vec{f}_i.\vec{n}) dS$$

Remark:
The spurious component appears explicitly in the far-field expression whereas it is implicitly contained in the near-field expression. *It can be removed in the far-field approach only.*

Accounting for spurious phenomena:

2) Spurious decay of trailing vorticity

In computations, numerical smoothing dominates over physical dissipation as a cause of trailing vorticity decay in the far-field.

As a consequence, induced drag "apparently" decreases as the control volume for its integration extends downstream.

If the area affected by this spurious transfer from one form of drag (induced) to another (viscous) can be identified, the quantity of drag transferred can be computed and used as a correction to the induced drag.

AIRBUS ONERA DLR

Modifications to the basic van der Vooren formulation for the far-field drag componen

1) Theoretically equivalent formulation (van der Vooren & Destarac):

$$D_v = -\int_{V_V} div\vec{f}_i dV \qquad D_w = -\int_{V_W} div\vec{f}_i dV \qquad D_i = \int_{V_V+V_W} div\vec{f}_i dV + D_p + D_f$$

2) Modified formulation for an easier implementation:

$$\vec{f}_i^* = -\rho(u - u_\infty - \Delta\overline{u})\vec{q} - (p - p_\infty)\vec{i}$$

$$D_v = -\int_{V_V} div\vec{f}_i^* dV + D_f \qquad D_w = -\int_{V_W} div\vec{f}_i^* dV \qquad D_i = \int_{V_V+V_W} div\vec{f}_i^* dV + D_p$$

$$(D_{vp} = -\int_{V_V} div\vec{f}_i^* dV)$$

Far-field drag extraction (ONERA-*ffd70*) from hybrid grid computations (DL TAU)

AIAA DPW-2: F6-WB/WBPN configurations

Table 1: Configurations, grid dimensions and aerodynamic conditions.

Configuration	Grid refinement	Nodes	Elements	M	CL	$Re_{\overline{c}}$
WB	level 3	8,750,330	24,469,766	0.75	0.50	3.10^6
WBPN	level 3	12,321,068	33,245,816	0.75	0.50	3.10^6
WBPN	level 2	8,202,568	21,824,379	0.75	0.50	3.10^6
WBPN	level 2	8,202,568	21,824,379	0.75	0.60	3.10^6

Table 2: Drag breakdown: numerical results. Drag coefficients expressed as drag counts (1 drag count = 10^{-4}).

		near-field (TAU)			far-field (TAU+*ffd70*)			
Configuration	Grid	CD_p	CD_f	CD_p+CD_f	CD_v	CD_w	CD_i	$CD_v+CD_w+CD_i$
WB	level 3	161.0	125.3	286.3	188.6	1.3	89.6	279.5
WBPN	level 3	178.9	149.1	328.0	226.3	4.8	89.6	320.7
WBPN	level 2	179.9	149.1	329.0	227.7	4.8	89.2	321.7
WBPN	level 2	235.4	146.9	382.3	235.5	14.0	125.2	374.7

Integration volumes for viscous drag (grey) and wave drag (yellow) extracti

F6-WBPN configuration. DLR-TAU computation. Hybrid grid, level 3. M=0.75 CL=0.5 $Re_c=3.10^6$

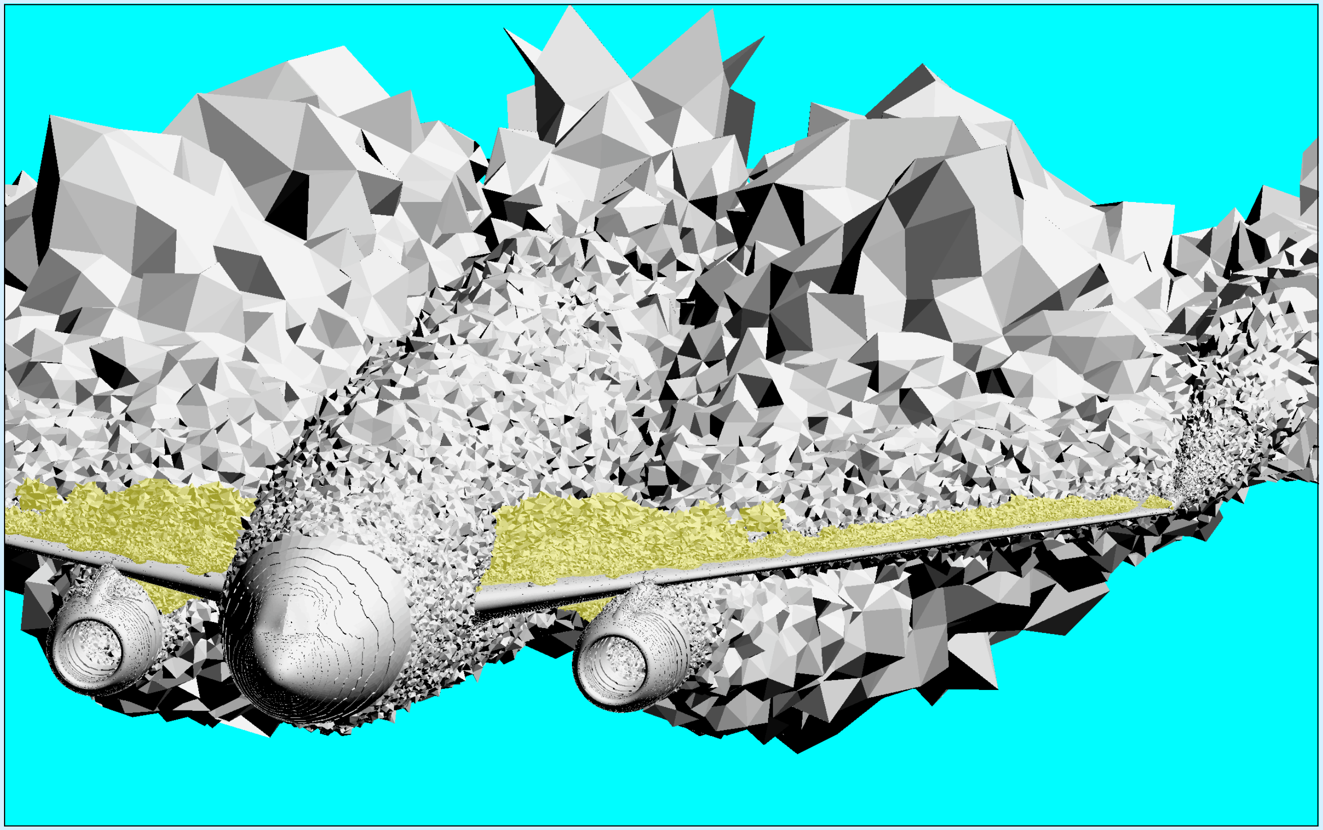

Integration volumes for viscous drag (grey) and wave drag (yellow) extracti

F6-WBPN configuration. DLR-TAU computation. Hybrid grid, level 3. M=0.75 CL=0.5 Re_c=3.10^6

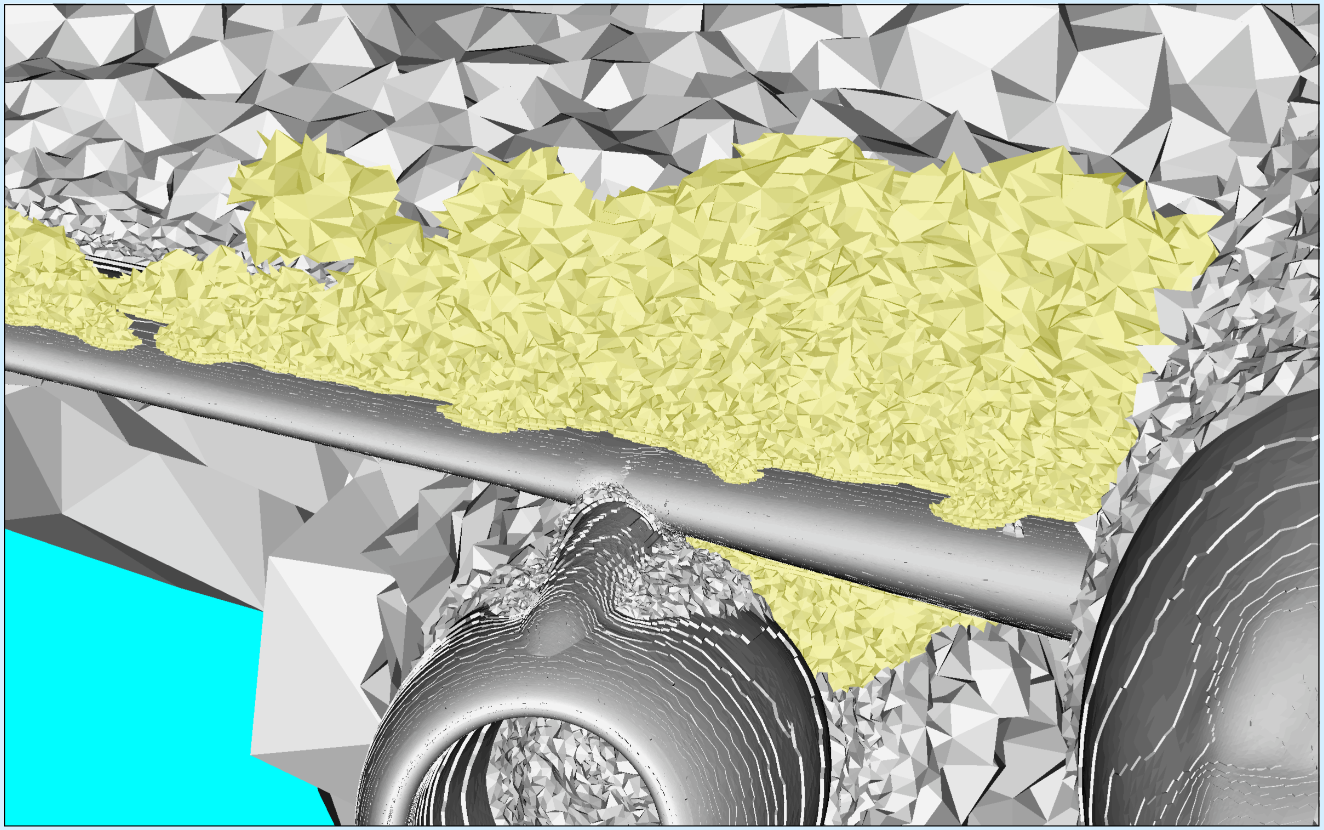

Spanwise drag distributions

F6-WB/WBPN configurations. DLR-TAU computations. Hybrid grids, level 3. M=0.75 CL=0.5 Re$_c$=3

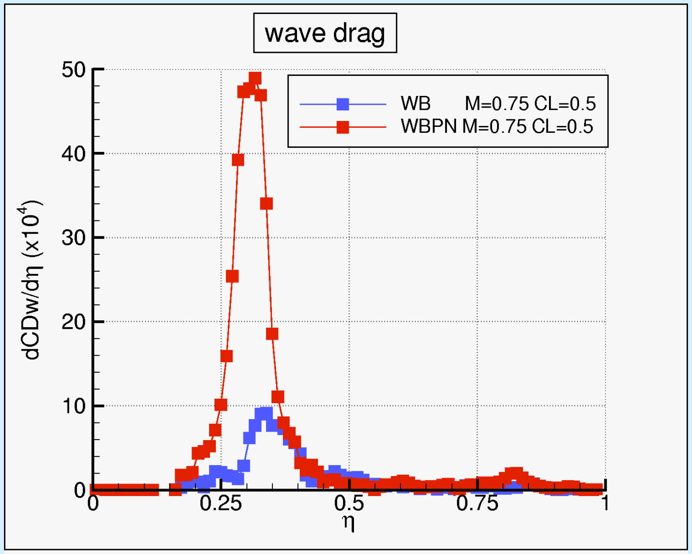

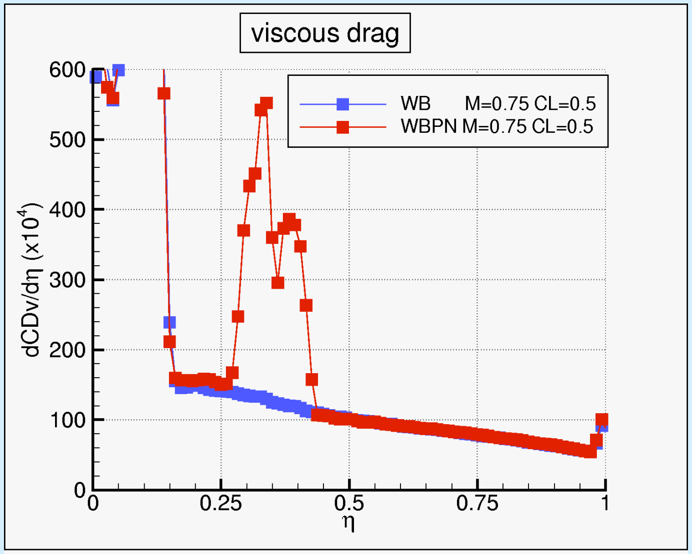

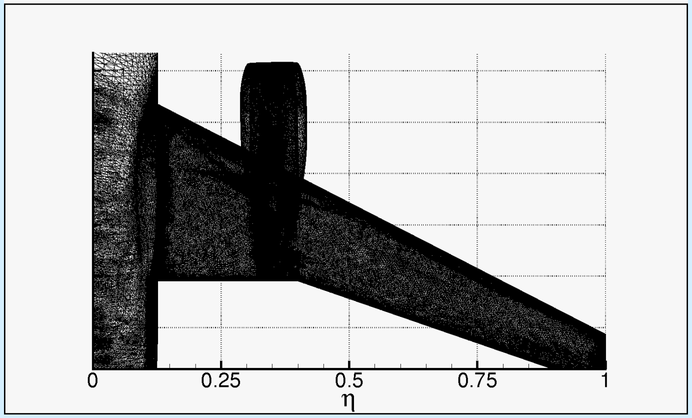

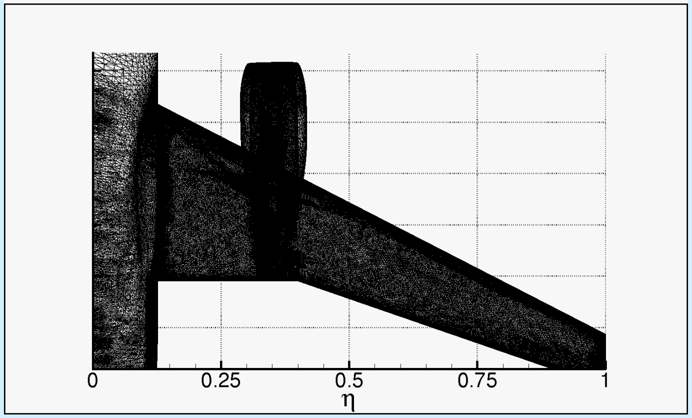

Spanwise drag distributions

F6-WBPN configuration. DLR-TAU computations. Hybrid grid, level 2. M=0.75 CL=0.5/0.6 Re_c=3.10

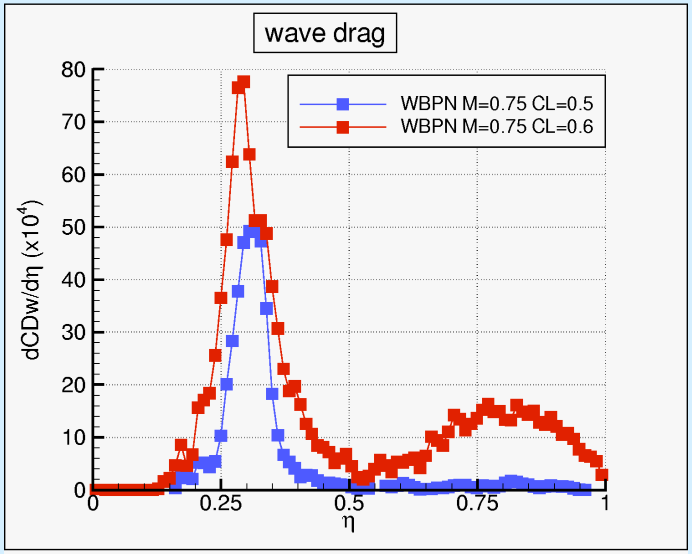

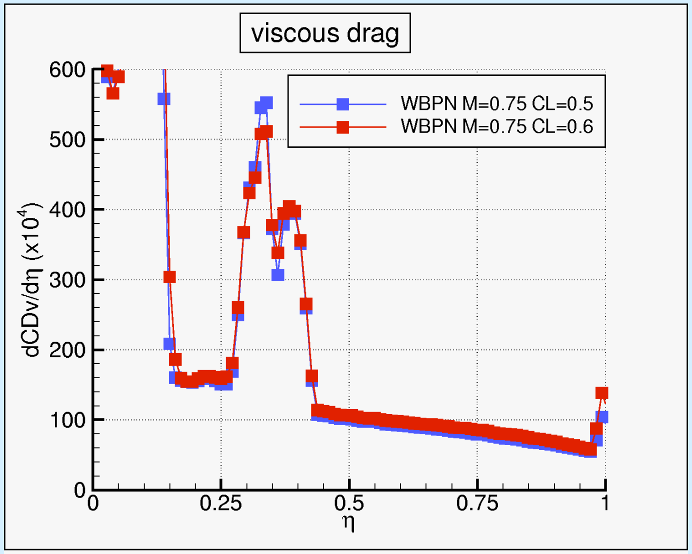

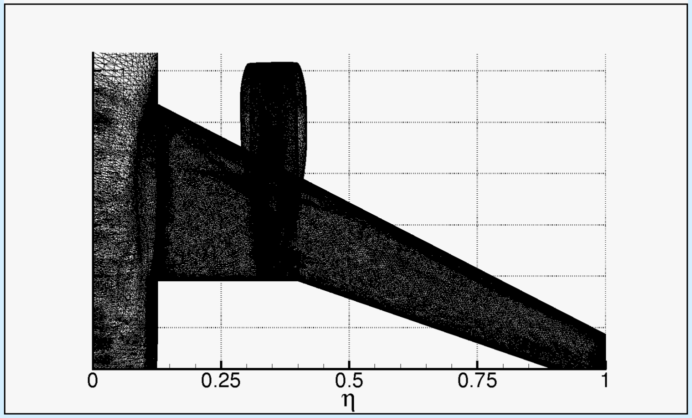

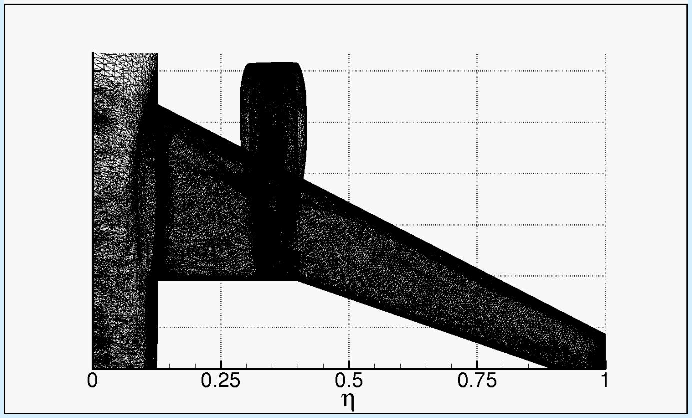

Spanwise wave drag distributions

F6-WBPN configuration. DLR-TAU computations. Hybrid grid, level 2. M=0.75 CL=0.5/0.6 Re_c=3.10

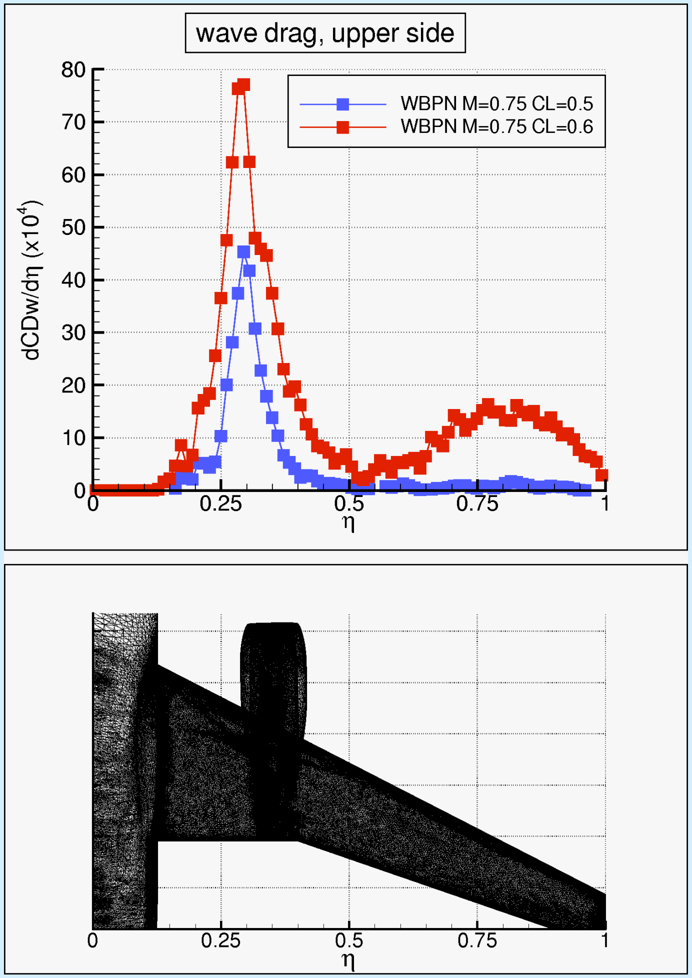

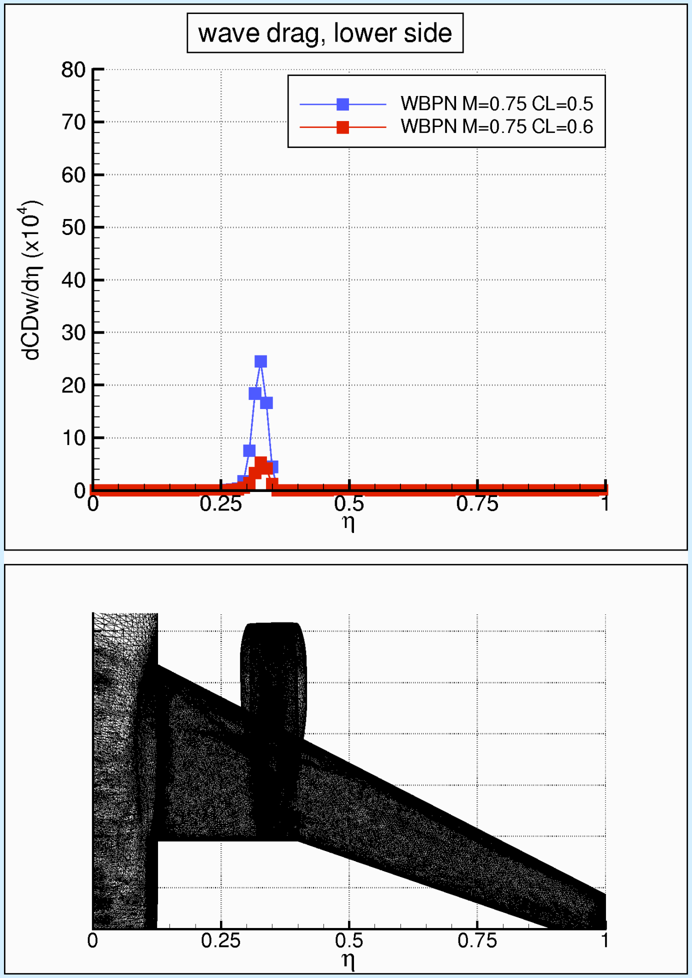

Elimination of spurious drag sources in the far-field drag extraction

F6-WBPN configuration. DLR-TAU computation. Hybrid grid, level 3. M=0.75 CL=0.5 $Re_c=3.10^6$

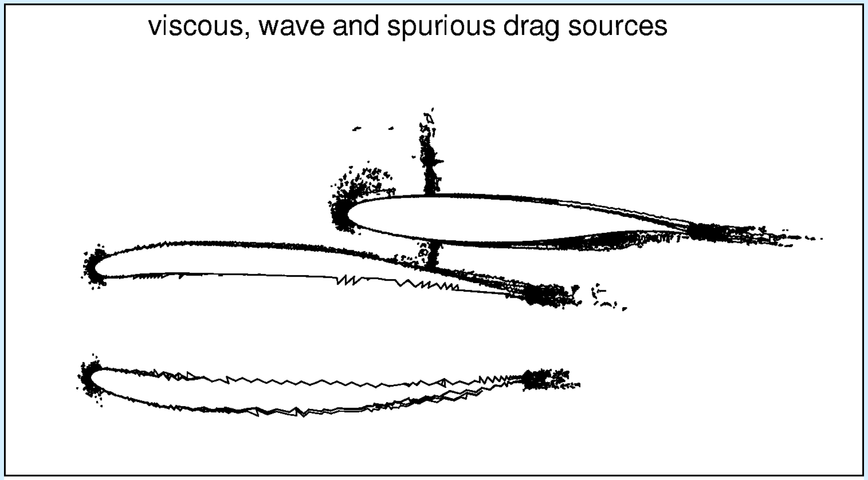

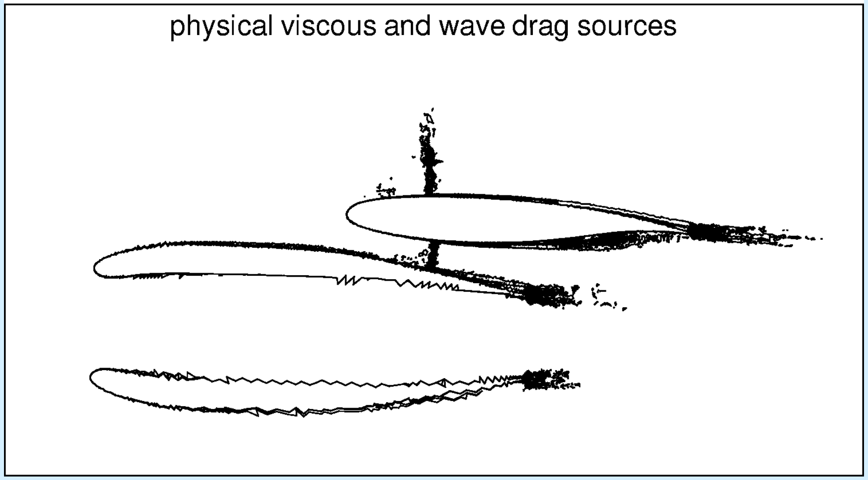

Concluding remarks

➪ *Drag can be extracted from a numerical solution either in the near-field or in the far-field.*

➪ *Far-field drag extraction provides <u>physical</u> and <u>local</u> information about the sources of drag.*

These additional information are very useful in aerodynamic design.

➪ *In the far-field analysis, spurious drag sources can be detected and eliminated. Far-field drag may thus be more accurate than near-field drag.*

The localisation, visualisation and evaluation, of the spurious drag sources in the field also provide useful <u>numerical</u> information about the quality of the grid and/or computation.